J|A|C|S
ARTICLES

Published on Web 07/17/2009

Monoiron Hydrogenase Catalysis: Hydrogen Activation with the Formation of a Dihydrogen, Fe−$H^{\delta-}\cdots H^{\delta+}$−O, Bond and Methenyl-$H_4MPT^+$ Triggered Hydride Transfer

Xinzheng Yang and Michael B. Hall*

Department of Chemistry, Texas A&M University, College Station, Texas 77843-3255

Received April 3, 2009; E-mail: mbhall@tamu.edu

Abstract: A fully optimized resting state model with a strong Fe−$H^{\delta-}\cdots H^{\delta+}$−O dihydrogen bond for the active site of the third type of hydrogenase, [Fe]-hydrogenase, is proposed from density functional theory (DFT) calculations on the reformulated active site from the recent X-ray crystal structure study of C176A (Cys176 was mutated to an alanine) mutated [Fe]-hydrogenase in the presence of dithiothreitol. The computed vibrational frequencies for this new active site model possess an average error of only ±4.5 cm^{-1} with respect to the wild-type [Fe]-hydrogenase. Based on this resting state model, a new mechanism with the following unusual aspects for hydrogen activation catalyzed by [Fe]-hydrogenase is also proposed from DFT calculations. (1) Unexpected dual pathways for H_2 cleavage with proton transfer to Cys176−sulfur or 2-pyridinol's oxygen for the formation and regeneration of the resting state with an Fe−$H^{\delta-}\cdots H^{\delta+}$−O dihydrogen bond before the appearance of methenyl-H_4MPT^+ (MPT^+). (2) The strong dihydrogen bond in this resting state structure prevents D_2/H_2O exchange. (3) Only upon the arrival of MPT^+ with its strong hydride affinity can D_2/H_2O exchange take place as the arrival of MPT^+ triggers the breaking of the strong Fe−$H^{\delta-}\cdots H^{\delta+}$−O dihydrogen bond by taking a hydride from the iron center and initiating the next H_2 (D_2) cleavage. This new mechanism is completely different than that previously proposed (*J. Am. Chem. Soc.* **2008**, *130*, 14036) which was based on an active site model related to an earlier crystal structure. Here, Fe's role is H_2 capture and hydride formation without MPT^+ while the pyridone's special role involves the protection of the hydride by the dihydrogen bond.

Introduction

With only abundant base metals (Fe and Ni) in their active sites, hydrogenases hold out hope for future application of hydrogen as a clean, high efficiency, and low-cost energy carrier.[1] Three phylogenetically unrelated hydrogenases, [NiFe]-, [FeFe]-, and [Fe]-hydrogenases, have been found to catalyze the formation and consumption of H_2 in the biological environment. Their structures and catalytic mechanisms are attracting increasing attention and being applied to the development of efficient synthetic catalysts for hydrogen-fueled processes. Among these hydrogenases, the H_2-forming methylenetetrahydromethopterin dehydrogenase (Hmd, iron−sulfur cluster-free hydrogenase, or [Fe]-hydrogenase), which catalyzes the reversible reduction of N^5,N^{10}-methenyl-tetrahydromethanopterin (methenyl-H_4MPT^+, or MPT^+) with H_2 to N^5,N^{10}-methylene-tetrahydromethanopterin (methylene-H_4MPT, or HMPT) and a proton (eq 1), was discovered by Thauer and co-workers in *Methanothermobacter marburgensis* only two decades ago.[2]

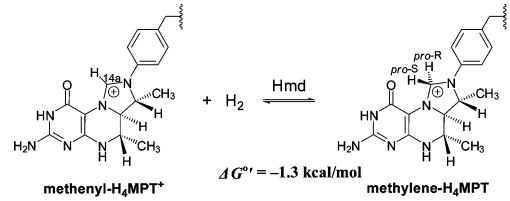

(1)

Hmd also catalyzes a direct exchange of the *pro*-R hydrogen of MPT with the protons of water.[3] It differs from the dimetal hydrogenases in that the purified enzyme *per se* does not catalyze the conversion of *para*-H_2 to *ortho*-H_2 or the isotopic H_2/D_2O exchange reaction. These reactions specifically require the presence of MPT^+. Based on the first crystal structure of the active site (Scheme 1A) of wild-type Hmd,[3] we proposed a catalytic mechanism,[4] where the arrival of substrate (MPT^+) triggered the electron release from the pyridone ligand and allowed cleavage of H_2 between Fe and MPT^+. The triggering of a change in the pyridone donor strength explained why the isotopic D_2/H_2O exchange catalyzed by Hmd is strictly dependent on the presence of MPT^+ and the formation of H_4MPT.

In a more recent study of the active site structure of Hmd, Hiromoto et al. crystallized a C176A (Cys176 was mutated to an alanine) mutated Hmd with dithiothreitol (DTT) and observed

(1) (a) Armstrong, F. A.; Fontecilla-Camps, J. C. *Science* **2008**, *321*, 498. (b) Kubas, G. J. *Chem. Rev.* **2007**, *107*, 4152. (c) Vignais, P. M.; Billoud, B. *Chem. Rev.* **2007**, *107*, 4206. (d) Fontecilla-Camps, J. C.; Volbeda, A.; Cavazza, C.; Nicolet, Y. *Chem. Rev.* **2007**, *107*, 4273. (e) De Lacey, A. L.; Fernández, V. M.; Rousset, M.; Cammack, R. *Chem. Rev.* **2007**, *107*, 4304. (f) Vincent, K. A.; Parkin, A.; Armstrong, F. A. *Chem. Rev.* **2007**, *107*, 4366. (g) Siegbahn, P. E. M.; Tye, J. W.; Hall, M. B. *Chem. Rev.* **2007**, *107*, 4414.

(2) Zirngibl, C.; Hedderich, R.; Thauer, R. K. *FEBS Lett.* **1990**, *261*, 112.

(3) Shima, S.; Pilak, O.; Vogt, S.; Schick, M.; Stagni, M. S.; Meyer-Klaucke, W.; Warkentin, E.; Thauer, R. K.; Ermler, U. *Science* **2008**, *321*, 572.

(4) Yang, X.; Hall, M. B. *J. Am. Chem. Soc.* **2008**, *130*, 14036.

Scheme 1[a]

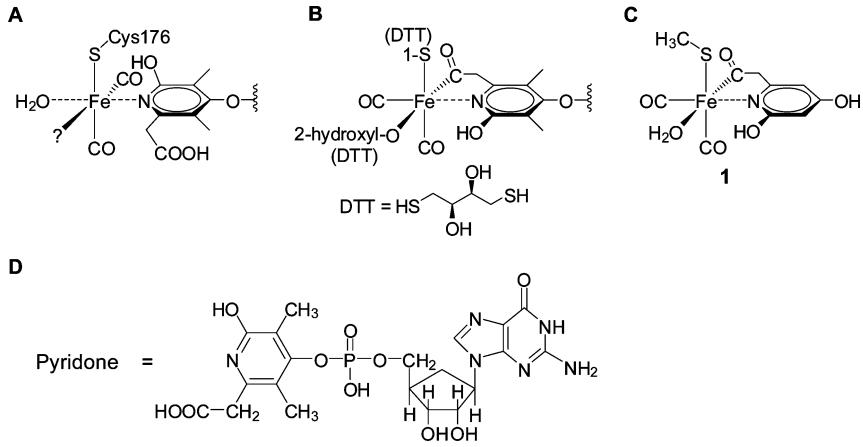

[a] (A) The first interpreted crystal structure of the active site of Hmd. The unknown ligand is "?". (B) Reinterpreted active site structure of Hmd from crystallized C176A mutation with DTT. (C) New model for the wild-type Hmd based on (B). (D) Structure of the guanylylpyridone (in its 2-pyridinol tautomeric form).[3]

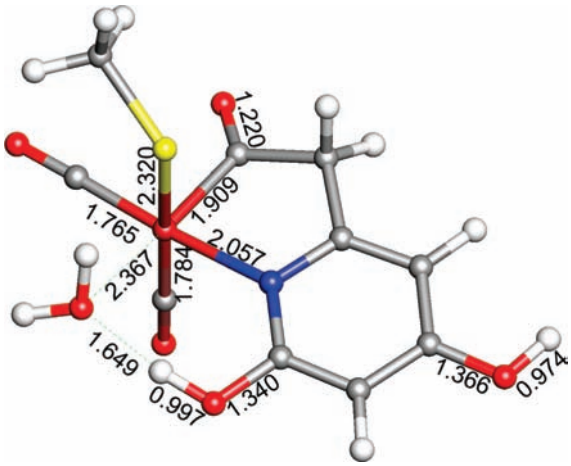

Figure 1. Optimized new active site model structure of **1**. Bond lengths are in angstrom.

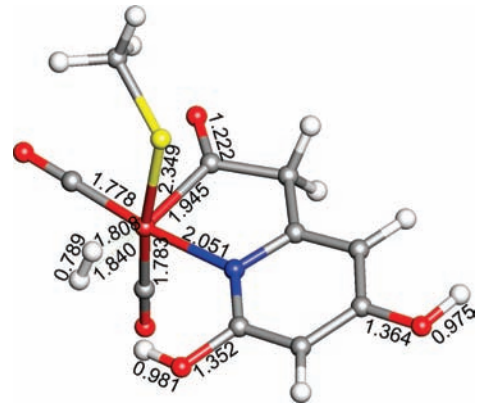

Figure 2. Optimized structure of **2** after H_2O/H_2 substitution. Bond lengths are in angstrom.

a different active site structure, in which the iron atom has a pseudo-octahedral coordination with a DTT-sulfur, a DTT-oxygen, a CO and the 2-pyridinol's acyl-carbon in a plane, and the other CO and the 2-pyridinol's nitrogen *trans* to each other (Scheme 1B).[5] Based on this crystal structure, Hiromoto et al. reinterpreted the active site structure of the wild-type Hmd. They believe that "the previous interpretation of the electron density was biased by the lack of imagination concerning the possibility of an acyl group as iron ligand and on the subsequent conclusion that the orientation of a negatively charged carboxylate group towards the rather unpolar protein interior is unlikely".[5] Furthermore, the new structure could be closer to wild-type Hmd because it was mutated but grown in vivo while the original structure was assembled in vitro. Herein, we compute a new reaction mechanism that is based on this new model for the active site structure of Hmd (Scheme 1C and **1** in Figure 1). Our previously proposed "trigger" mechanism for the catalytic hydrogen activation by Hmd was based on the crystal structure which indicated two open sites. However, in the new active site structure, the pyridone is bidentate and the H_2O binding position is changed from *trans* to the pyridone N to *cis* to the pyridone N, which is now the only open position for H_2O/H_2 exchange and H_2 activation in this new model. The calculated absolute energies of **1** and the previous model cannot be compared directly because the CH_2COOH group on pyridone in the previous model is revised as CH_2CO in **1**. To verify the stability of **1**, we optimized the structure of an isomer of it in which the positions of H_2O and CO *trans* to N are switched (so the coordination of H_2O and CO groups are similar to that of the old model). This isomer is 10.7 kcal/mol less stable than **1** in electronic energy. The new catalytic mechanism for the hydrogen activation catalyzed by Hmd proposed in this study is therefore completely different from the previous one and has several unusual aspects.

Computational Details

All calculations were performed using Tao−Perdew−Staroverov−Scuseria[6] (TPSS) functional with an all-electron 6-31++G(d,p) basis set within the Gaussian 03 suite of *ab initio* programs.[7] There are some arguments about the reliability of the B3LYP functional on transition metal complex calculations in recent

(5) Hiromoto, T.; Ataka, K.; Pilak, O.; Vogt, S.; Stagni, M. S.; Meyer-Klaucke, W.; Warkentin, E.; Thauer, R. K.; Shima, S.; Ermler, U. *FEBS Lett.* **2009**, *583*, 585.

(6) Tao, J. M.; Perdew, J. P.; Staroverov, V. N.; Scuseria, G. E. *Phys. Rev. Lett.* **2003**, *91*, 146401.

(7) Frisch, M. J. et al. *Gaussian 03, revision E.01 suite of programs for ab initio calculation*; Gaussian, Inc.: Wallingford, CT, 2004.

Scheme 2. Formation of Resting State **3** with an Fe−H$^{\delta-}$···H$^{\delta+}$−O Dihydrogen Bond through the Cleavage of H_2 by Cys176−Sulfur

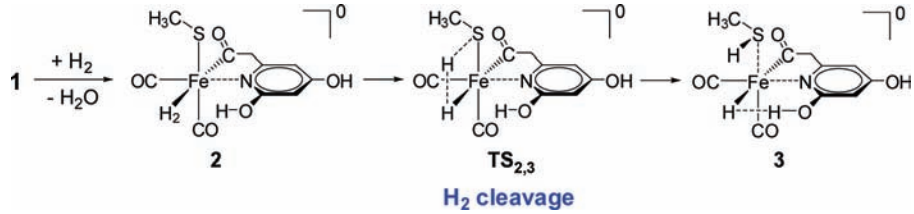

Scheme 3. Mechanism for Hydrogen Activation Catalyzed by Hmd Showing Unexpected Dual Pathways for H_2 Cleavage with Proton Transfer to Cys176-Sulfur (**2** → **3**) and 2-Pyridinol's Oxygen (**7** → **3**), the formation of Fe−H$^{\delta-}$···H$^{\delta+}$−O Dihydrogen Bond in **3**, and the Hydride Transfer Triggered by MPT$^+$ (**4** → **5**)

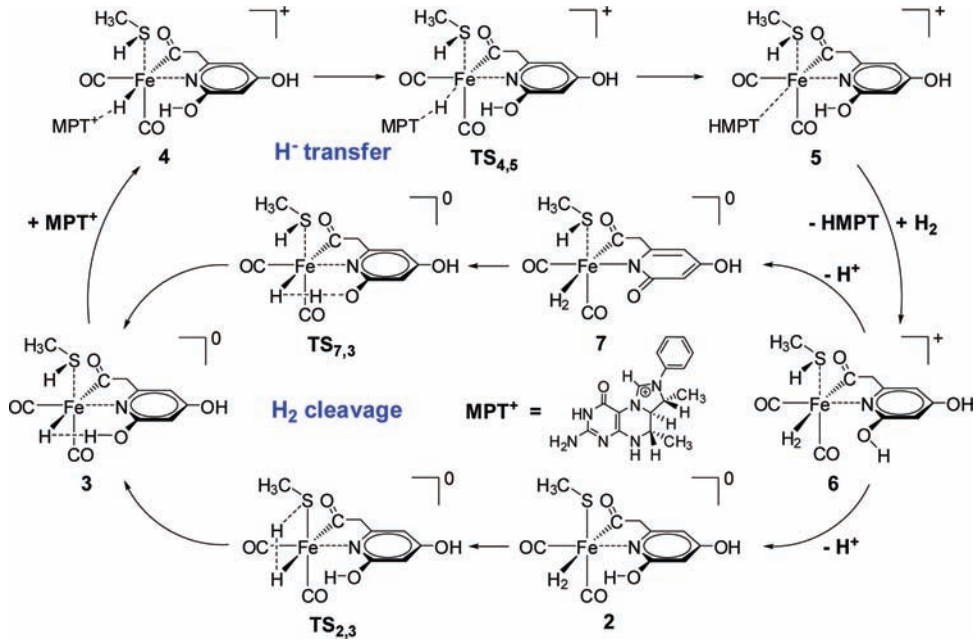

years.[8] The TPSS functional was selected for DFT calculations in this study because it is the only meta-GGA level functional without empirical parameters and has a much higher computational efficiency than hybride functionals. Its reliability for this system is evaluated in the Supporting Information. The geometric structures of all species were optimized as gas phase. Calculating the harmonic vibrational frequencies and noting the number of imaginary frequencies confirmed the nature of all intermediates (no imaginary frequency) and transition state structures (only one imaginary frequency). The latter were also confirmed to connect reactants and products by intrinsic reaction coordinate (IRC) calculations. The gas-phase free energies, G, were calculated at $T = 298.15$ K within the harmonic potential approximation at optimized structures. The effect of solvent was taken into account by single-point calculations on gas-phase optimized structures using an integral equation formalism polarizable continuum model (IEFPCM) for ether ($\epsilon = 4.335$ as a protein environment mimic). The 3D molecular structures displayed in this paper were drawn by using the JIMP2 program.[9]

Results and Discussion

The calculated solvent-corrected vibrational frequencies of the *cis*-$(CO)_2$ groups in **1** at the gas-phase optimized geometric structures are 2007 and 1947 cm^{-1}, lower than the gas-phase frequencies of 2014 and 1964 cm^{-1}, and very close to the observed absorption peaks of wild-type Hmd's resting state at 2011 and 1944 cm^{-1}.[10] These results confirm that the assumed spin and oxidative states are singlet Fe^{2+}. Unlike the previous active site model, which had two open sites, the H_2O binding position in **1** is the only open position for H_2O/H_2 exchange and further H_2 activation. The calculated endoergicity for H_2O/H_2 substitution (**1** → **2**, Figure 2) is only 12.9 kcal/mol when the same solvent (ether) is used for all species and 8.8 kcal/mol when water is used as solvent for H_2O and H_2 with $\epsilon = 78.39$. The actual H_2O/H_2 exchange barrier should be lower than this value because the solvent correction in current IEFPCM calculations cannot fully reflect the hydrogen bonding for this single H_2O becoming part of the bulk water environment. For example, the calculated solvent free energy correction for a single H_2O molecule in water is −6.8 kcal/mol, but the experimental value for a single H_2O becoming part of the bulk water environment is approximately −14 kcal/mol in free

(8) (a) Paier, J.; Marsman, M.; Kresse, G. *J. Chem. Phys.* **2007**, *127*, 024103. (b) Harvey, J. N. *Annu. Rep. Prog. Chem. Sect. C* **2006**, *102*, 203. (c) Sousa, S. F.; Fernandes, P. A.; Ramos, M. J. *J. Phys. Chem. A* **2007**, *111*, 10439. (d) Furche, F.; Perdew, J. P. *J. Chem. Phys.* **2006**, *124*, 044103.

(9) (a) Manson, J.; Webster, C. E.; Hall, M. B. *JIMP2, version 0.091, a free program for visualizing and manipulating molecules*; Texas A&M University: College Station, TX, 2006. (b) Hall, M. B.; Fenske, R. F. *Inorg. Chem.* **1972**, *11*, 768.

(10) Lyon, E. J.; Shima, S.; Boecher, R.; Thauer, R. K.; Grevels, F.-W.; Bill, E.; Roseboom, W.; Albracht, S. P. J. *J. Am. Chem. Soc.* **2004**, *126*, 14239.

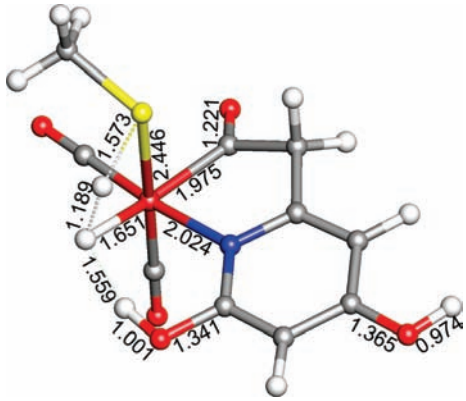

Figure 3. Optimized structure of transition state $\mathbf{TS_{2,3}}$ (785*i* cm^{-1}) for the cleavage of H_2 with sulfur as proton acceptor. Bond lengths are in angstrom.

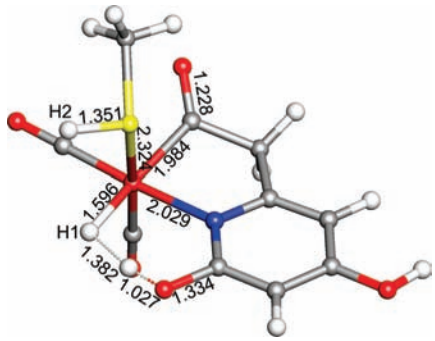

Figure 4. Optimized resting state structure of **3** with a strong $Fe-H^{\delta-}\cdots H^{\delta+}-O$ dihydrogen bond. Bond lengths are in angstrom.

energy.[11] Therefore, we assume H_2O/H_2 exchange is energetically neutral and presumably fairly rapid. As shown in Scheme 2, after H_2O/H_2 substitution, H_2 in **2** is split by Cys176-sulfur through transition state $\mathbf{TS_{2,3}}$ (Figure 3) with a free energy barrier of only 6.6 kcal/mol to form the resting state **3** (Figure 4), which is 3.4 kcal/mol more stable than **2** in free energy and has a strong $Fe-H^{\delta-}\cdots H^{\delta+}-O$ dihydrogen bond in it. The calculated solvent-corrected vibrational frequencies of *cis*-$(CO)_2$ in **3** at the gas-phase optimized geometric structures are 2007 and 1949 cm^{-1}, sufficiently close to those predicted for **1** that these two species would not be differentiated in IR experiments and the resting state of wild-typ Hmd could be either or both species.

Because of the low energy barrier of $\mathbf{TS_{2,3}}$, H_2 cleavage occurs very rapidly after H_2O/H_2 exchange to form the thermodynamically more favorable structure **3**. Interestingly, the observed Mössbauer spectra of Hmd shows no observable changes with the addition of H_2.[12] In the crystal structure study of the wild-type Hmd,[3] the holoenzyme was reconstituted and crystallized from the heterologously produced apoenzyme of *Methanocaldococcus jannaschii* with the labile iron guanylyl pyridone cofactor. The unknown ligand is more likely to be a water molecule because the electron density of this position was increased by a factor of 1.6 after the wild-type Hmd crystal was soaked with cyanide. However, in the Mössbauer spectroscopy study,[11] the purification of wild-type Hmd and the cofactor were performed under strictly anoxic conditions using

(11) Siegbahn, P. E. M.; Blomberg, M. R. A. *Computational modeling for homogeneous and enzymatic catalysis*; Morokuma, K., Musaev, D. G., Eds.; WILEY-VCH: 2008; pp 57−81.
(12) Shima, S.; Lyon, E. J.; Thauer, R. K.; Mienert, B.; Bill, E. *J. Am. Chem. Soc.* **2005**, *127*, 10430.

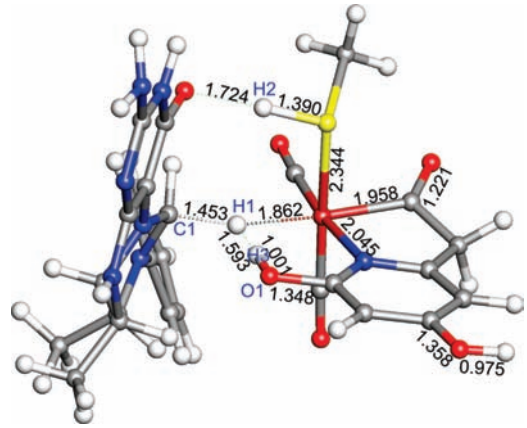

Figure 5. Optimized structure of transition state $\mathbf{TS_{4,5}}$ (697*i* cm^{-1}) for hydride transfer. Bond lengths are in angstrom.

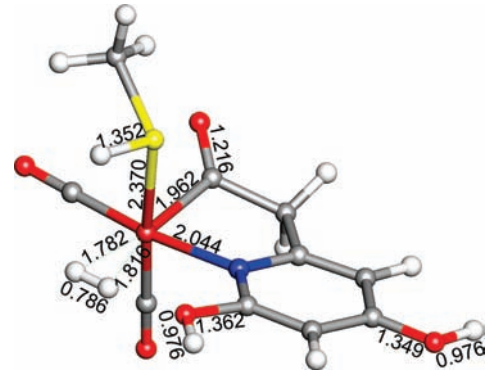

Figure 6. Optimized structure of **6**. Bond lengths are in angstrom.

an anaerobic chamber filled with 95% N_2 and 5% H_2 (v/v). Therefore, the resting state of Hmd in the Mössbauer study is more likely to be **3**, which is more stable and cannot react with additional H_2 or easily undergo D_2/H_2O exchange (see below for the analysis of the strength of the dihydrogen bond in **3**). In addition, the Mulliken charges of the Fe center in **2** (0.142) and **3** (0.138) are very close. Thus, the addition of H_2 in the Mössbauer study would have no observable effect on the measured Mössbauer spectra of Hmd if it was at **3**.

Beginning from the resting state **3**, the new mechanism for the hydrogen activation catalyzed by Hmd and hydride transfer triggered by MPT^+ is shown in Scheme 3. Upon arrival and formation of **4**, MPT^+ takes a hydride through a hydride transfer transition state $\mathbf{TS_{4,5}}$ (Figure 5) which is only 15.3 kcal/mol above **4** and generates the cation **6** (Figure 6) through HMPT/H_2 exchange. Once **6** is formed, dual pathways for H_2 cleavage are available. It can lose a proton either from S to regenerate **2** or from O to generate a new neutral complex **7** (Figure 7), which can also split H_2 and regenerate **3** through transition state $\mathbf{TS_{7,3}}$ (Figure 8). This unexpected H_2 cleavage mechanism differs from our previously proposed direct H_2 cleavage between Fe and MPT^+[4] and shows the importance of the Cys176-sulfur and the 2-pyridinol's oxygen in the hydrogen activation catalyzed by this type of hydrogenase. Although it might appear that D_2/H_2O exchange could occur in **3**, we will show that the strong $Fe-H^{\delta-}\cdots H^{\delta+}-O$ dihydrogen bond prevents the exchange at this point.

Because of the importance of H/D exchange processes in understanding the catalytic mechanism, the energetics of depro-

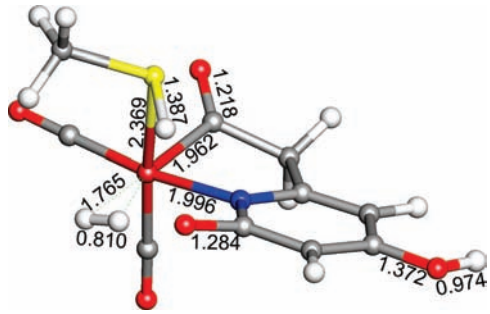

Figure 7. Optimized structure of **7**. Bond lengths are in angstrom.

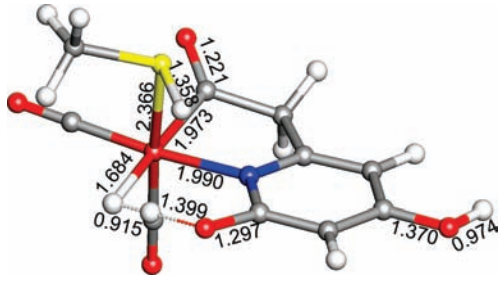

Figure 8. Optimized structure of $\mathbf{TS}_{7,3}$ ($531i$ cm^{-1}) for H_2 cleavage. Bond lengths are in angstrom.

Scheme 4. Thermodynamic Cycle Connecting Gas (g) and Solvated (s) Phase for the Calculation of Deprotonation Energies in Solvent

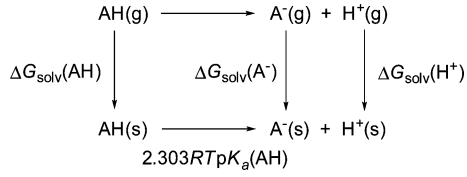

tonation of the intermediates in Scheme 3 must be evaluated before the analysis of the energy profile in this mechanism. The thermodynamic cycle connecting the gas and solvated (protein mimic) phase for the calculation of the deprotonation energy with solvent correction is shown in Scheme 4. The estimation of the free energies for the deprotonation of these complexes requires the value of the solvation free energy of the proton $\Delta G_{solv}(H^+)$, which can be calculated by using the following equation,

$$\Delta G_{solv}(H^+) = G_{gas}(AH) - G_{gas}(A^-) + \Delta G_{solv}(AH) - \Delta G_{solv}(A^-) + 2.303RT\mathrm{p}K_a \quad (2)$$

Unfortunately, this quantity is sensitive to the conditions, and the experimental values range from −252.6 to −271.7 kcal/mol.[13] According to the most recent investigation, the value of $\Delta G_{solv}(H^+)$ is in the range between −262 and −264 kcal/mol.[13,14] In the following evaluations, we chose $\Delta G_{solv}(H^+)$ as −262.5 kcal/mol, which is based on a recent estimate for substituted imidazoles[15] and is in the middle of the experimental range. To verify this value, we also calculated the $\Delta G_{solv}(H^+)$ in THF using a recent experimental pK_a value of Ph_3CH in THF (pK_a = 44)[16] and DFT (see the computational details above, THF for solvent effect correction) calculated results of $G_{gas}(Ph_3CH)$, $G_{gas}(Ph_3C^-)$, $\Delta G_{solv}(Ph_3CH)$, and $\Delta G_{solv}(Ph_3C^-)$. The calculated $\Delta G_{solv}(H^+)$ in THF is −262.0 kcal/mol. Therefore, −262.5 kcal/mol can be considered as a reliable value for the proton solvation free energy for our further analysis. Table 1 lists the calculated gas-phase free energies of deprotonations, $\Delta G_{gas}(-H^+)$, from S or O1 in **2**, **3**, **4**, **5**, **6**, and **7**, the total solvation free-energy (ΔG_{solv}), and the predicted total free energies for deprotonation in protein (ΔG_{tot}) based on the equation $\Delta G_{tot} = \Delta G_{gas}(-H^+) + \Delta G_{solv} + \Delta G_{solv}(H^+)$.[17]

Table 1. Predicted Free Energies (kcal/mol) for the Deprotonation of **2**, **3**, **4**, **5**, **6**, and **7** Using Experimentally Estimated $\Delta G_{solv}(H^+)$ = −262.5 kcal/mol[15]

deprotonation	$\Delta G_{gas}(-H^+)$	ΔG_{solv}[a]	ΔG_{tot}[b]
O1 of **2**	310.2	−27.4	20.3
O1 of **3**	330.7	−28.9	39.3
S of **3**	316.3	−28.6	25.2
S of **7**	313.3	−28.1	22.7
S of **4** (→ **8**)	263.2	15.6	16.3
S of **5** (→ **9**)	236.5	17.1	−8.9
O1 of **6** (→ **7**)	228.3	29.2	−5.0
S of **6** (→ **2**)	230.9	28.6	−3.0

[a] $\Delta G_{solv} = \Delta G_{solv}(A^-) - \Delta G_{solv}(AH)$ in ether. [b] $\Delta G_{tot} = \Delta G_{gas}(-H^+) + \Delta G_{solv} + \Delta G_{solv}(H^+)$.

According to the estimated deprotonation free energies listed in Table 1, the neutral complexes **2**, **3**, and **7** need at least 20 kcal/mol to lose a proton. Deprotonation of O1 in **3** requires almost 40 kcal/mol of free energy, reflecting the strong interactions between the hydrogen atoms in the $Fe-H^{\delta-}\cdots H^{\delta+}-O$ dihydrogen bond of **3**. Deprotonation of S in **3** needs more than 25 kcal/mol of free energy. Therefore, these deprotonation reactions are unlikely under mild conditions. Among these neutral complexes, the deprotonation from the O1 atom in **2** is the easiest. However, if intermediate **2** was to lose this proton and form an anion complex, the simultaneously formed $Fe-H^{\delta-}\cdots H^{\delta+}-O$ dihydrogen bond will protect these remaining H atoms from isotopic D_2/H_2O exchange. In contrast to **2**, **3**, and **7**, deprotonation of the cations **5** and **6** are several kcal/mol downhill in free energy.

In addition to the calibrated free energies of deprotonations, the energetic response of movement of the cation MPT^+ from the exterior to the interior of the protein environment is important to obtain the correct relative free energies of the intermediates and transition states for the entire catalytic cycle. Although a rather large model for MPT^+ (Scheme 3) is used in our calculations, it is still much smaller than the real structure of MPT^+, and the implicit solvent free-energy corrections cannot

(13) am Busch, M. S.; Knapp, E.-W. *Chem. Phys. Chem.* **2004**, *5*, 1513.
(14) (a) Kelly, C. P.; Cramer, C. J.; Truhlar, D. G. *J. Phys. Chem. B* **2007**, *111*, 408. (b) Kelly, C. P.; Cramer, C. J.; Truhlar, D. G. *J. Phys. Chem. B* **2006**, *110*, 16066. (c) Tissandier, M. D.; Cowen, K. A.; Feng, W. Y.; Gundlach, E.; Cohen, M. J.; Earhart, A. D.; Coe, J. V. *J. Phys. Chem. A* **1998**, *102*, 7787.
(15) Topol, I. A.; Tawa, G. J.; Burt, S. K.; Rashin, A. A. *J. Phys. Chem. A* **1997**, *101*, 10075.
(16) Abdur-Rashid, K.; Fong, T. P.; Greaves, B.; Gusev, D. G.; Hinman, J. G.; Landau, S. E.; Lough, A. J.; Morris, R. H. *J. Am. Chem. Soc.* **2000**, *91*, 9155.
(17) The estimated value of $\Delta G_{solv}(H^+)$ is slightly variable and depends on the solvent so its effective value in the protein environment is not accurately known. The value of $\Delta G_{solv}(H^+)$ is important for the evaluation of $\Delta G_{solv}(MPT^+)$ and the rate determining steps of **3** → **5** or **3** → **9**. However, according to the equation for the calculation of total deprotonation free energy (Table 1), $\Delta G_{solv}(H^+)$ does not effect the differences of deprotonation free energies between the complexes listed in Table 1. D_2/H_2O exchange still cannot happen because of the strong $Fe-H^{\delta-}\cdots H^{\delta+}-O$ dihydrogen bond and the nature of the rate-determining step should not change.

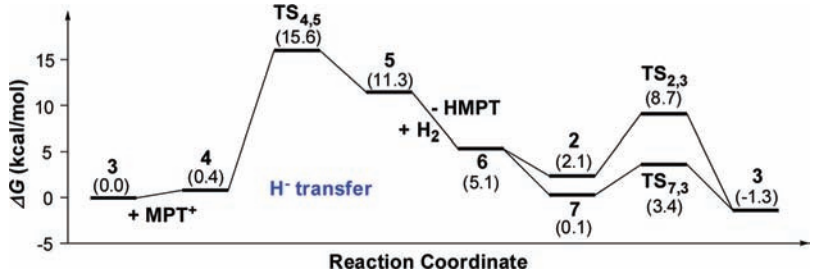

Figure 9. Relative free energy profile for the hydrogen activation mechanism shown in Scheme 3.

Scheme 5. Catalytic Cycle for Hydrogen Activation Mechanism with Hydride Transfer after the Deprotonation of **4**[a]

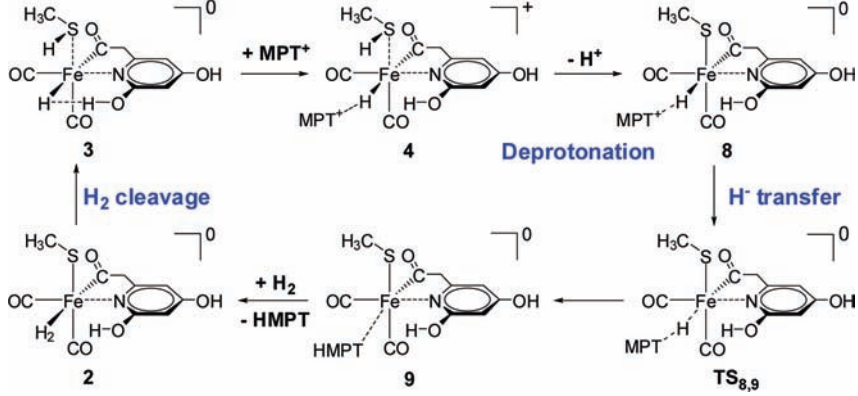

[a] The attack of MPT^+ makes proton loss from S of **4** easier.

fully correct for the differential free energy in this movement, especially because of a variety of van der Waals and electrostatic interactions neglected in this small model. Fortunately, it is known that the protein binds MPT^+ and the free energy for the Hmd catalyzed reversible reduction of MPT^+ with H_2 to HMPT and H^+ has been measured experimentally as $\Delta G^{\circ\prime} = -1.3$ kcal/mol (eq 1).[18] Therefore, based on eq 1 and the estimated experimental values of $\Delta G^{\circ\prime}$ and $\Delta G_{solv}(H^+)$, the unidentified attractive features of the protein can be described through a calibrated solvent correction for MPT^+, $\Delta G_{solv}(MPT^+)$, by the following equation,

$$\Delta G_{solv}(MPT^+) = G_{gas}(HMPT) + \Delta G_{solv}(HMPT) + \Delta G_{solv}(H^+) - G_{gas}(H_2) - \Delta G_{solv}(H_2) - G_{gas}(MPT^+) - (\Delta G^{\circ\prime}) \quad (3)$$

which yields a calibrated $\Delta G_{solv}(MPT^+)$ of -17.7 kcal/mol. Here the calculated $\Delta G_{solv}(H_2)$ is 2.0 kcal/mol in ether. Since H_2 probably comes from water, $\Delta G_{solv}(H_2)$ in water ($\epsilon = 78.39$) is also calculated and a value of 2.4 kcal/mol is obtained. With only a 0.4 kcal/mol difference for ether and water, the effect of a different solvent on $\Delta G_{solv}(H_2)$ can be neglected and the value obtained with ether as solvent is used in further analysis for consistency. Accordingly, a reaction coordinate with relative free energies for the entire catalytic mechanism can be determined as shown in Figure 9.

There are two main steps following the formation of **3**, hydride transfer and H_2 cleavage. With the calibrated value for $\Delta G_{solv}(MPT^+)$, **4** is only 0.4 kcal/mol higher than **3** in free energy. This low barrier means MPT^+ can attach to the active site of Hmd easily, as observed in the experiment. The carbocation character of the methenyl C14a of MPT^+ makes it an excellent hydride acceptor. The transition state $\mathbf{TS_{4,5}}$ for the transfer of hydride (the rate-determining step) from the iron center to MPT^+ for the formation of HMPT is only 15.2 kcal/mol higher than **4** in free energy. The total free energy barrier of this catalytic cycle is 15.6 kcal/mol. Once HMPT is formed in **5**, it leaves the active site and another H_2 molecule enters to fill the vacant position and form the intermediate cation **6**, which can lose a proton easily from either S or O1 to regenerate the neutral complexes **2** and **7** which are 3.0 and 5.0 kcal/mol more stable, respectively. Then **3** is regenerated through H_2 cleavage transition state $\mathbf{TS_{2,3}}$ (Figure 3) and ready for next catalytic cycle. Here we would like to point out that the total free energy barrier of this catalytic mechanism is based on the estimated experi-

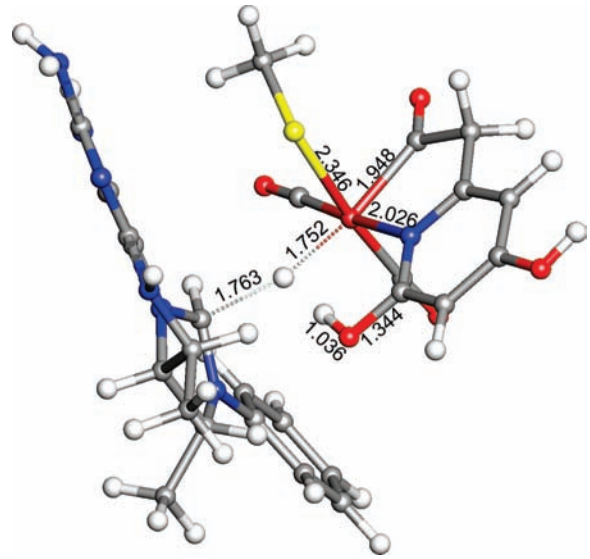

Figure 10. Optimized structure of transition state $\mathbf{TS_{8,9}}$ ($465i$ cm^{-1}) for hydride transfer. Bond lengths are in angstrom.

(18) Thauer, R. K.; Klein, A. R.; Hartmann, G. C. *Chem. Rev.* **1996**, *96*, 3031.

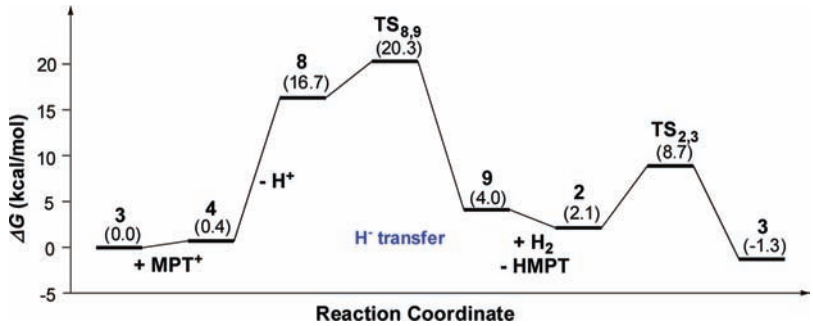

Figure 11. Relative free energy profile for the hydrogen activation mechanism shown in Scheme 5.

mental value of $\Delta G_{solv}(H^+)$ and $\Delta G^{\circ\prime}$. The total free energy barrier (**TS$_{4,5}$**) relative to **3** increases/decreases with the decrease/increase of $\Delta G_{solv}(H^+)$ and is therefore less accurate than the pure reaction energies calculated, which are independent of $\Delta G_{solv}(H^+)$.

In the dual-pathway H_2 cleavage step, **TS$_{2,3}$** is only 6.6 kcal/mol higher than **2**, and **TS$_{7,3}$** is only 3.3 kcal/mol higher than **7** in free energy. Since O1 and S can split H_2 easily, it might seem that the isotopic D_2/H_2O exchange catalyzed by this active site model would not be dependent on the presence of MPT^+, a prediction in conflict with the observed phenomena.[3] However, H_2 cleavage is fast and the species created, **3**, is quite stable with a H1···H3 distance of only 1.38 Å, much shorter than typical $M-H^{\delta-}\cdots H^{\delta+}-N$ dihydrogen bonds of 1.7−1.9 Å,[19] which indicates the existence of an especially strong $Fe-H^{\delta-}\cdots H^{\delta+}-O$ dihydrogen bond in **3**. A similar but weaker $Fe-H^{\delta-}\cdots H^{\delta+}-O$ dihydrogen bond has been predicted in the study of [FeFe]-hydrogenase.[20] The strong interactions between Fe, H1, H3, and O1 protect the hydrogen atoms from direct H/D exchange with D_2O in **3** and prevent the vibrational coupling of H1 and *cis*-$(CO)_2$. This explains why **1** and **3** have almost the same vibrational frequencies for the *cis*-$(CO)_2$. The predictions for the free energies required for the deprotonation of these structures (see above) show the strength of the $Fe-H^{\delta-}\cdots H^{\delta+}-O$ dihydrogen bond in **3**. This strength protects these H-atoms from participating in D_2/H_2O exchange reactions. Although H_2 could exchange with D_2 at this point the dihydrogen bond prevents the exchange with water. The arrival of MPT^+, a strong hydride acceptor, triggers the breaking of the dihydrogen bond and species like **4** and **5** could be long-lived enough and thermodynamically available for exchange of active site H(D) with water. Thus, the arrival of MPT^+ allows D_2/H_2O exchange which occurs in (**4** ⇌ **5** ⇌ **6**).

Although Scheme 3 shows a route from **5** → **6** → **2** or **7**, the proton could be lost first from **4** before the generation of **5**. Due to the attack of MPT^+, the deprotonation of S in cation **4** is much easier than in **3** and needs only 16.3 kcal/mol of free energy, which is close to the hydride transfer barrier of **TS$_{4,5}$** and can easily be achieved under mild conditions. Therefore, as shown in Scheme 5, there may be a second reaction pathway for the hydride transfer to MPT^+ beginning with the deprotonation of **4** followed by hydride transfer from the neutral complex **8** through transition state **TS$_{8,9}$** (Figure 10). The calculated relative free energies of the intermediates and transition states in Scheme 5 based on the calibrated $\Delta G_{solv}(MPT^+)$ of −17.7 kcal/mol are shown in Figure 11. The rate-determining step is transition state **TS$_{8,9}$**, the hydride transfer again. Hydride transfer from the neutral complex **8** is much easier than that from cation **4** as **TS$_{8,9}$** is only 3.6 kcal/mol higher than **8**. The total free energy barrier of **TS$_{8,9}$** is 20.3 kcal/mol, 4.7 kcal/mol higher than **TS$_{4,5}$**, but still achievable under mild conditions. Note that a specific base could lower the free energy of **8** such that this pathway would have an even lower overall free-energy barrier than the first pathway. Once the hydride is transferred from the iron center to MPT^+, $HMPT/H_2$ exchange occurs and **2** is formed. Then, the resting state **3** is regenerated through the low barrier H_2 cleavage transition state **TS$_{2,3}$** (Figure 3) and ready for the next catalytic cycle. The −1.3 kcal/mol difference in the free energies of **3** at the start and the end in Figures 9 and 11 reflects the experimental free energy difference driving this catalytic reaction (eq 1), which was used to calibrate the solvent free energy of MPT^+ (eq 3).

Conclusion

A fully optimized resting state model with a strong $Fe-H^{\delta-}\cdots H^{\delta+}-O$ dihydrogen bond for the active site of the third type of hydrogenase, [Fe]-hydrogenase, is proposed from DFT calculations on the reformulated active site from the recent X-ray crystal structure study of C176A mutated [Fe]-hydrogenase in the presence of dithiothreitol.[5] The computed vibrational frequencies for this new active site model possess an average error of only ±4.5 cm^{-1} with respect to the measured absorption peaks of wild-type [Fe]-hydrogenase. The strong dihydrogen bond in this resting state structure prevents D_2/H_2O exchange. Only upon the arrival of MPT^+ with its strong hydride affinity can D_2/H_2O exchange take place, as the arrival of MPT^+ triggers the breaking of the strong $Fe-H^{\delta-}\cdots H^{\delta+}-O$ dihydrogen bond by taking a hydride from the iron center and initiating the next H_2 (D_2) cleavage. In the new mechanism, Fe's role is H_2 capture and hydride formation while the pyridone's special role involves the protection of the hydride by the dihydrogen bond. Meanwhile, H_2 is split through an unexpected dual-pathway cleavage mechanism with proton transfer to Cys176-sulfur and 2-pyridinol's oxygen for the formation and regeneration of the resting state with an $Fe-H^{\delta-}\cdots H^{\delta+}-O$ dihydrogen bond. The proposed catalytic mechanism for hydrogen activation by [Fe]-hydrogenase helps our understanding of the catalytic nature of hydrogenases and may provide ideas for novel catalyst design for

(19) (a) Crabtree, R. H.; Siegbahn, P. E. M.; Eisenstein, O.; Rheingold, A. L.; Koetzle, T. F. *Acc. Chem. Res.* **1996**, *29*, 348. (b) Peris, E.; Lee, J. C., Jr.; Rambo, J. R.; Eisenstein, O.; Crabtree, R. H. *J. Am. Chem. Soc.* **1995**, *117*, 3485.

(20) Fan, H.-J.; Hall, M. B. *J. Am. Chem. Soc.* **2001**, *123*, 3828.

hydrogenation catalysts, for low cost, high efficiency hydrogen production, and for hydrogen release from hydrogen storage materials.[21]

Acknowledgment. We acknowledge financial support from NSF (CHE-0518074, CHE-0541587, and DMS-0216275) and The Welch Foundation (A-0648). We thank S. Shima and R. K. Thauer for informative discussions on the crystal structure and spectroscopy of [Fe]-hydrogenase.

Supporting Information Available: Complete ref 7, evaluation of density functionals, atomic coordinates of optimized stationary points and transition states. This material is available free of charge via the Internet at http://pubs.acs.org.

JA902689N

(21) (a) Yang, X.; Hall, M. B. *J. Am. Chem. Soc.* **2008**, *130*, 1798. (b) Yang, X.; Hall, M. B. J. Organomet. Chem. 2009, in press, doi: 10.1016/j.jorganchem.2009.04.018.